Structural, microstructural and electrical properties of Lanthanum (La^{+3}) modified Lead iron niobate $Pb(Fe_{0.5}Nb_{0.5})O_3$.

Thesis submitted in partial fulfillment
of the requirements for the degree of

Master of Science (M.Sc.)

in

Department of Physics

Under the academic Autonomy

National Institute of Technology, Rourkela

by

Shreenu Pattanaik

(Roll No-410PH2141)

Under the guidance of

Dr. Dillip K Pradhan

Department of Physics
National Institute of Technology, Rourkela
Rourkela-769008, Odisha, India.

Department of Physics
National Institute of Technology, Rourkela
Rourkela-769008, Orissa, India.

Certificate

This is to certify that the work in the thesis entitled "***Structural, microstructural and electrical properties of Lanthanum (La^{+3}) modified Lead iron niobate $Pb(Fe_{0.5}Nb_{0.5})O_3$.***" submitted by **Miss. Shreenu Pattanaik** is a record of an original research work carried out by her under my supervision and guidance in partial fulfillment of the requirements for the award of the degree of Master of Science in Physics. Neither this thesis nor any part of it has been submitted for any degree or academic award elsewhere.

Dr. Dillip K Pradhan
Asst. Professor
Department of Physics,
National Institute of Technology, Rourkela-769008

DECLARATION

I hereby declare that the work carried out in this thesis is entirely original. It was carried out by me along with Mr Soumya Ranjan Dash at Department of Physics, National Institute of Technology, Rourkela. I further declare that it has not formed the basis for the award of any degree, diploma, or similar title of any university or institution.

Shreenu Pattanaik

Roll No- 410PH2141

Department of physics

National Institute of Technology

Rourkela-769008

Acknowledgment

I express my sincere gratitude to my supervisor Dr.Dillip K Pradhan for his valuable guidance and support in carrying out this project. I would like to acknowledge all the faculties of the Department of Physics for their help and support. I extend my thanks to all my colleagues and Ph.D. scholar Mr.Satya Narayan Tripathy for his co-operation. I would also like to thank Soumya Ranjan Dash for his valuable help. Finally, I would like to acknowledge Director, NIT Rourkela for permitting me to carry out this project successfully and also for providing the essential facilities.

Shreenu Pattanaik

Department of Physics

NIT, Rourkela

Rourkela-769008

Contents Pages

Abstract

One series of lanthanum-modified Lead iron niobate ceramic oxides having chemical formula $Pb_{(1-x)}La_x(Fe_{0.5}Nb_{0.5})_{(1-x/4)}O_3$ (x=0.00, 0.02, 0.04, 0.06, 0.08) ceramics were prepared by mixed oxide high temperature solid state reaction route. Preliminary structural, microstructural and electrical properties of the compounds were studied using XRD, SEM and complex impedance spectroscopic analysis. The formations of the compounds were confirmed by XRD analysis. From preliminary structural using the XRD data, the lattice parameters are calculated using standard IUCR software CHECKCELL. Williamson Hall method was used for finding the crystallite size in the samples. Microstructures/morphology of the materials was analyzed by scanning electron microscopy. Dielectric and impedance spectroscopic properties of the materials were studied in a wide frequency range at different temperatures. The temperature dependent dielectric constant showed the ferroelectric to praelectric phase transition around 115^0C for $Pb(Fe_{0.5}\ Nb_{\ 0.5})O_3$. Then with increase in La concentration, there is a decrease in the transition temperature and above 4% La concentration, the transition temperature is below the room temperature.

Chapter-1

Introduction

1.1 Ferroelectric Materials:

Ferroelectric materials have attracted the attention of the scientific community since last few decades for its fundamental physics and potential device applications. The phenomenon of ferroelectricity was discovered in 1921 by Valsek in Rockchell salt [1]. A breakthrough in the research on ferroelectric materials came in the 1950's, leading to the widespread use of barium titanate ($BaTiO_3$) based ceramics in capacitor applications and piezoelectric transducer devices. Since then, many other ferroelectric ceramics including lead titanate ($PbTiO_3$), lead zirconate titanate (PZT), lead lanthanum zirconate titanate (PLZT), and relaxor ferroelectrics like lead magnesium niobate (PMN) have been invented, studied and utilized for a variety of potential device applications. With the development of ceramic processing and thin film technology, many new device applications have emerged. The biggest use of ferroelectric ceramics has been in the areas such as dielectric ceramics for capacitor application, ferroelectric thin film for non-volatile memories, piezoelectric materials. Hence lot of research work was carried out both experimental and theoretical – in this field in the past 4 to 5 decades [2].

Ceramics are defined as the solid compounds that consist of metallic and non-metallic elements which are formed by the application of heat and pressure. The most important properties of the ceramics are wear-resistant, brittle, refractory, thermal insulators, electrical insulators, nonmagnetic, oxidation resistance, and thermal shock prone and chemically stable. The nature of bonding between the atoms and type of atoms represents the properties of the

materials. Two most common chemical bonds for ceramic materials are covalent and ionic bonding. In comparison to metals, ceramics have very low electrical conductivity [3].

Most of the ceramic materials are dielectrics which possess very low electrical conductivity but supports electrostatic field. Electrical conductivity of ceramics depends on temperature and frequency. This is due to the reason that charge transport mechanisms are frequency dependent and thermal energy provides the activation energy for the charge migration. In general, ceramic materials have high dielectric strength and high dielectric constant for potential device applications.

1.2 Characteristics feature of the ferroelectric materials

(1) Lack of center of symmetry.

(2) Ferroelectric crystals must be piezoelectric though the converse is not true.

(3) Ferroelectric materials have one or more Curie temperature.

(4) Ferroelectric transitions are structural transitions.

(5) Ferroelectric materials obey Curie-Weiss law.

(6) Ferroelectric materials exhibits hysteresis loop

The ferroelectrics are characterized by the ferroelectric hysteresis loop, i.e., the polarization P is a double-valued function of the applied electric field E. Typical polarization – electric field hysteresis loop displayed by ferroelectrics. As the electric field is high enough, all the ferroelectric domains are aligned in the direction of field, the crystal becomes monodomain and the polarization is saturated. The extrapolation of the linear portion of the curve at high field back to the polarization axis represents the value of the spontaneous polarization P_s. When the electric field is removed, most of the domains remain aligned and the crystal still exhibit

polarization. The polarization at zero fields after saturation is called remnant polarization P_r. The remnant polarization can be removed when a field in the opposite direction is applied and reaches a critical value. The strength of the electric field required to reduce the polarization to zero is called the coercive field E_c.

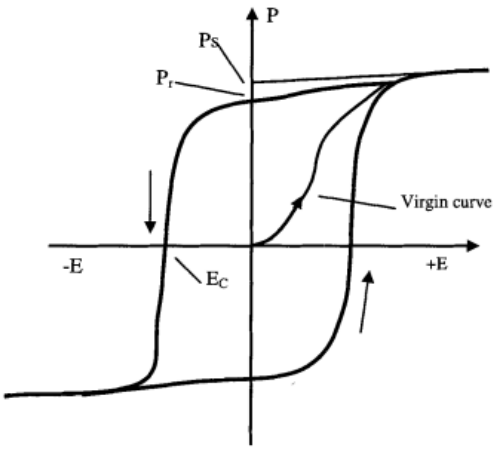

(Figure-1Typical Ferroelectric hysteresis loop)

1.3 Types of ferroelectric materials:

Ferroelectric materials existed can be divided in to following categories:

- Corner Sharing Octahedra
  - (1) Perovskites (ABO_3)
  - (2) Pyrochloro ($A_2B_2O_7$)
  - (3) Tungsten Bronze type Compounds ($(A_1)_2(A_2)_4(C)_4(B_1)_2(B_2)_8O_{30}$)
  - (4) Bismuth Oxide Layer Structured Ferroelectrics ($(Bi_2O_2)^{+2}$, $(A_{n-1},B_n\ O_{3n-1})^{-2}$)
- compounds containing hydrogen bonded radicals
- organic polymers
- ceramic polymer composites

1.4 Perovskite structure

The perovskite structure, of chemical formula ABX_3, consists of two distinct cation sites (A and B) and one anion site (C). Crystals of the prototypical perovskite, $CaTiO_3$, were first discovered in 1839. However, halide and sulfide perovskites are also known and of technological interest [Bennett 2009]. A-site can be monovalent, divalent or trivalent and B-site can be pentavalant, tetravalent or trivalent .The coordination number of A-site cation is 8 to 10 and B-site cation is 6.The structures of perovskites are determined by short range attractive (bonding) and repulsive forces between nearby ions, as well as long range electrostatic interactions between unit cells. Composition determines the balance of these forces, and therefore the structure. The stability of peroskite is represented by tolerance factor (t) and determines the property of the perovskite [4].

$$t = \frac{(R_A + R_O)}{\sqrt{2}(R_B + R_O)}$$

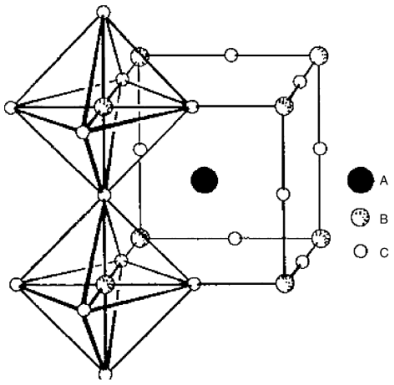

(Figure-2 Typical Perovskite structure)

(1) $t \geq 1$, for ferroelectric perovskites, $BaTiO_3$, $PbTiO_3$ and $KNbO_3$,

(2) $t < 1$ for antiferroelectric perovskites $PbZrO_3$, $NaNbO_3$ and $BiFeO_3$.

(3) t=1 corresponds to an ideal perovskite

While a t<1 Indicates tilting or rotation of the BO6 octahedral and for t>1 a displacive distortion within the BO_6 octahedral.

1.5 Ferroelectric Phase Transition

The transition from ferroelectric (less-symmetric or distorted structure) to paraeletric (high-symmetric centrosymmetric) phase in most of the times is accompanied by a structural or crystallographic phase transition. In modern language phase transition quite often referred to symmetry breaking. The phase transition in a ferroeletric material is usually of two types

(1) Displacive phase transition

(2) Order-disorder phase transition

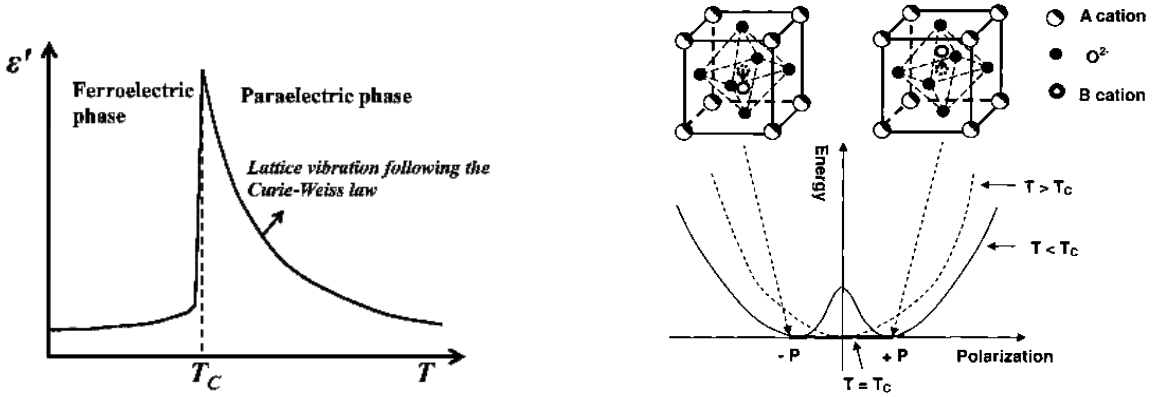

(Figure-3 Structural phase transition)

Displacive transitions proceed through a small distortion of the bonds (dilatational or rotational). As the key for the ferroelectricity, Ps arises due to the non-concidence of the positive and negative charge centers in the unit cell. Ferroelecity primarily results from the off center displacement of the B cation in ABO_3 peroskite structure leading to displacive phase transition. This off center displacement in the peroskite ferroelerics is the result of competition between the short range repulsion force between adjacent electron clouds of ions, which favours the non ferroeletric centrosymmetric structure and additional bonding between B cation and oxygen ions. Order-disorder transitions proceed through substitution between atoms possibly followed by small atomic displacements. They are commonly found in metals and alloys and in ceramics [5].

Order Parameter

Most phase transitions are characterized by the appearance of some non-zero quantity in the ordered state and the same varnishes in the disorder state. Such quantity is called order parameter.

Normally, one encounters two type of phase transition according to order parameter.

(1) First order phase transition, characterized by the appearances of latent heat, finite change in volume and hysteresis. (First derivative of Gibb's free energy is discontinuous.)

(2) A second order phase transition, characterized by discontinuity in the specific heat. (First derivative of Gibb's free energy is discontinuous.)

It is well known that order parameter is a decreasing function of temperature and must varnish at critical temperature. If the order parameter varnishes discontinuously at Tc, then the transition is said to be first order while if it varnished continuously, it is called second order. Near the Curie point or phase transition temperature, thermodynamic properties including dielectric, elastic, optical, and thermal constants show an anomalous behavior. This is due to the distortion in the crystal as the phase changes. The temperature dependence of the dielectric constant above the Curie point ($T>T_C$) in most of the ferroelectric crystals is governed by the Curie-Weiss law:

$$\varepsilon = \varepsilon_0 + \frac{C}{T - T_0}$$

Where, ε is the permittivity of the material, ε_0 is the permittivity of the vacuum, C is the Curie constant and T_0 is the Curie-Weiss temperature. In general the Curie-Weiss temperature T_0, is different from the Curie temperature T_C. For first order transitions, $T_0 < T_C$ while for

second order phase transitions, $T_0 = T_C$.

Complex perovskite type ferroelectrics with distorted cation arrangements show DPT (diffuse phase transition) which is characterized by a broad maximum for the temperature dependence of dielectric constant (ε) and dielectric dispersion in the transition region. For DPT, ε follows modified temperature dependence Curie Weiss law.

$$\varepsilon = \varepsilon_0 + \frac{C}{(T - T_m)^{\upsilon}}$$

where, T_m is the temperature at which ε reaches maximum (ε_m), C is the modified Curie constant and γ is the critical exponent. The γ factor explains the diffusivity of the materials, which lies in the range $1<\gamma<2$. In case of γ equals to unity, normal Curie–Weiss law is followed and it shows the normal ferroelectric phase transition.

1.6 Lead Iron Niobate and related materials

Lead iron niobate $Pb(Fe_{0.5}Nb_{0.5})O_3$ (PFN) is a lead based complex perovskite which is of great interest for multilayer capacitors owing to its high dielectric constant discovered by Smolenskii et al. PFN having a monoclinic structure, and a Curie temperature of 114 °C, therefore becomes a possible candidate for making new relaxor ferroelectrics exhibiting attractive piezoelectric properties. Recently it has been proposed that certain complex perovskite ferroelectric compounds. $A(B_I B_{II})O_3$ type, containing transition metal as one of the B cations, exhibit magnetic ordering through indirect exchange-mechanism. It has been studied ceramic powders, single crystal and also thin films. Raymond *et al.* extensively studied

the structural, thermoelectric, dieletric and impedance spectroscopic studies of lead iron niobate [6]. Wang *et al.* showed the enhanced dielectric properties in 0.94PFN-0.06PT single crystals [7]. Kumar *et al*. studied the enhanced electrical properties of PFN thin films. Mishra *et al.* reported the dieletric relaxation and magnetic properties of the PFN ceramics [8]. Sahoo *et al.* studied the effect of $V5^{+}$ and Y^{+3} substitutions on dieletric and ferroelectric properties of PFN [9]. Varshney *et al.* reported the dieletric properties of Ba^{2+} modified lead iron niobate [10].

Based on the literature survey, some of the main problems in PFN based material are

(1) Difficult to synthesize single phase PFN material. For example, when synthesized using conventional solid-state synthesis route, a pyrochlore phase ($Pb_3Nb_4O_{13}$ or $Pb_2Nb_2O_7$ type) with lower dielectric constant always coexists with the desired perovskite phase in PFN ceramics[11].

(2) PFN ceramics or similar iron-doped systems, the occurrence of Fe^{2+} and oxygen vacancies originated during the sintering process increase electrical conductivity, large frequency dispersion of dielectric constants , dielectric loss, space-charge accumulation at the grain boundary, all of them inhibition to optimal device performance. PFN ceramics also exhibit lower resistivity, for example, makes it almost impossible to pole PFN ceramics to determine the piezoelectric constants as well as to measure the polarization hysteresis characteristics[6].

Among the various methodologies available in literature, one of the important methods to solve the above mention problems is suitable substitutions. In the present study, we have planned to substitute La at the Pb-site of the complex perovskite PFN.

1.6 Materials under investigation:

$Pb_{(1-x)}La_x(Fe_{0.5}\ Nb_{0.}5)_{1-x/4}O_3$ (x=0.0, 0.02, 0.04, 0.06, 0.08)

1.7 Main Objectives:

The following will be the main objectives of the proposed work.

(1) Preparation of new complex ferroeletric compounds using high temperature solid state reaction route.

(2) Studies of the structural & micro-structural properties of the materials.

(3) Studies of dielectric responses as a function of frequency & temperature.

(4) Studies of Impedance and conductivity studies of the sample.

Chapter-2

Experimental Technique

In this chapter, the basic principles and various experimental techniques used in this work are briefly discussed. The characterization techniques include structural analysis, surface morphology study and dielectric measurements.

2.1Introduction

Ceramic materials are important class of in material science because of their direct and indirect application to solid-state device application and day to day life. Eventually synthesis of these materials is of a greater importance to the progress of material science. There are several method for synthesis of ceramic materials such as solid state reaction route, high energy ball milling (top to bottom approach), soft chemical route (bottom to top approach). To achieve a qualitative product with respect to purity, homogeneity, reactivity each method is having its own advantages and disadvantages. In this view, solid-state reaction route is found to be easier and low cost method by means of performance and economy.

2.2Solid State reaction route

The solid-state reaction route is the most widely used method for the preparation of polycrystalline solids from a mixture of solid starting materials. Solids do not react together at room temperature over normal time scales and it is necessary to heat them to much higher temperatures The factors on which the feasibility and rate of a solid state reaction include, reaction conditions, structural properties of the reactants, surface area of the solids, their reactivity and the thermodynamic free energy change associated with the reaction. In addition, the higher temperature allows some movement or flow of atoms through the solid at a

sufficient rate so that the desired product can eventually be obtained. A number of procedures are used to reduce the time needed for synthesis. The starting materials are often intimately grinded together, thus ensuring good mixing and hence increasing contact between the reacting grains.

Experimental Details

Polycrystalline powder of $Pb_{(1-x)}La_x(Fe_{0.5}Nb_{0.5})_{1-x/4}O_3$ (x=0.0, 0.02, 0.04, 0.06, 0.08) were synthesized by a conventional solid-state reaction route. The high purity oxides (PbO, Fe_2O_3, Nb_2O_5, La_2O_3,) (LOBA Chemie Private Limited, Mumbai, India) of required precursors were weighed according to the stoichiometric ratios and mixed by agate mortar and pestle for 2 hours then in wet (acetone) medium to obtain a homogeneous mixture for 4 hrs. 3% extra PbO was taken in order to compensate lead loss at high temperature. The dried mixture was put in alumina crucible and calcined at temperature 900 ^{O} C for 6 hours in furnace. The above heated powder formed into a lump and it was grinded till it became fine powder. Phase formation was checked by XRD at room temperature. The above calcined powder was mixed with 6% PVA (polyvinyl alcohol) as a binder in mortar and pestle. The binder mixed powder was compacted to form pellet by a hydraulic press at 6 x 10^{7} kg/m 2 pressure using 10mm die set. The sintering of the pellet sample was carried out at an optimized temperature of 1000 ^{O}C . The sintered pallets were polished by emery paper and painted with silver paste as an electrode for electrical measurement.

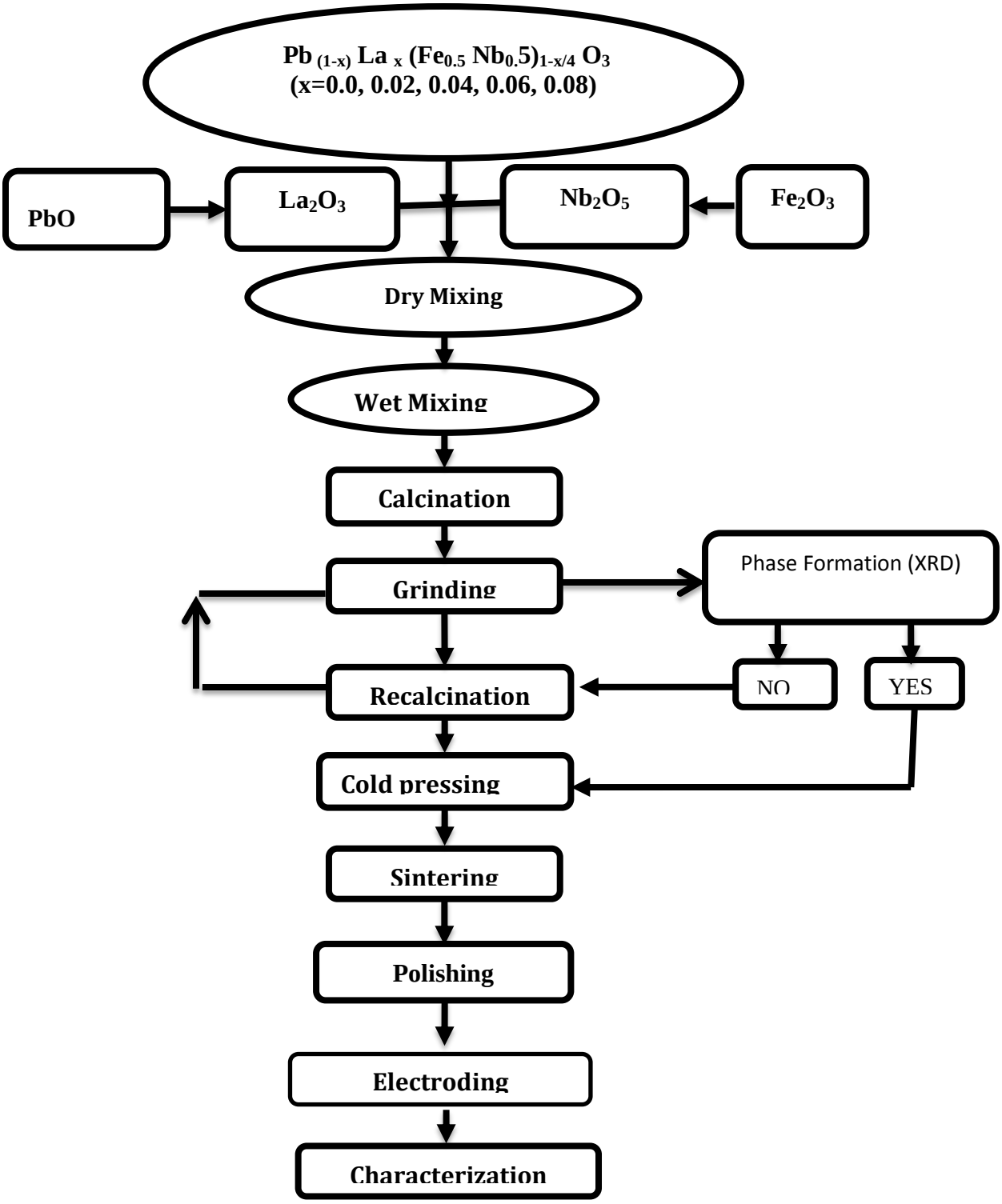

Flow chart for the preparation of ceramic samples by a solid-state reaction technique.

2.3 Characterization Technique

X-ray powder diffraction

X-ray diffraction is a (XRD) powerful non-destructive technique to characterize, analyze and interpret the detailed structural study of the compound. It predicts the quantative phase analysis as well as qualitative structural and microstructural analysis. X-rays are used to produce the diffraction pattern because their wavelength λ is typically the same order of magnitude that of the spacing *d* between planes in the crystal. In the present study we have recorded XRD-pattern in PAnalytic diffractometer.

The diffraction satisfies the Bragg equation,

$$2d\sin\theta = n\lambda$$

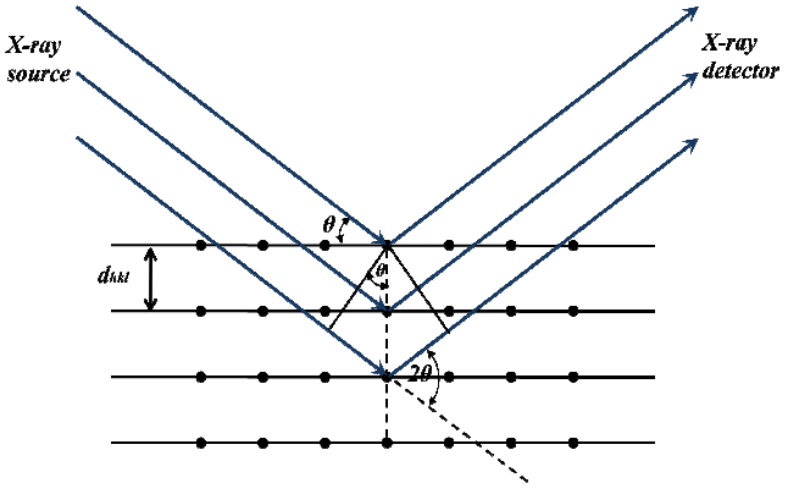

(Figure-1 Bragg's reflection from crystallographic planes)

Here *d* is the spacing between diffracting planes, θ is the incident angle, *n* is any integer, and λ is the wavelength of the beam.

The information in an XRD pattern is a direct result of three things:

(1) The size and shape of the unit cells, which determine the relative positions of the diffraction peaks.

(2) 2Atomic positions within the unit cell, which determine the relative intensities of the diffraction peaks electron (charge density distribution)

(3) Peak broadening is related to microstructural parameters (crystallite size, r.m.s strain and dislocation density)

It is impossible to find two different materials having same x-ray diffraction pattern. Therefore it can be used as *fingerprint* to identify the material[13-14].

The determination of lattice constants from the line positions or d spacing can be found from a general formula

$$\frac{1}{d_{hkl}^2} = V^2\ h^2b^2c^2\sin^2\alpha + k^2c^2a^2\sin^2\beta + l^2a^2b^2\sin^2\gamma$$

Where; V = volume of the unit cell

$$= abc\ 1 - \cos^2\alpha - \cos^2\beta - \cos^2\gamma + \cos\alpha\cos\beta\cos\gamma\ ^{1/2}$$

Here **a, b, c, α, β** and **γ** are lattice parameters and **h, k, l** are the miller indices. The above formula is used to calculate lattice parameters for all the compositions.

The microstructural parameters crystallite size (**D**) and strain can be related by Williamson-Hall equation.

$$\beta\ Cos\theta = 4ЄSin\theta + \lambda/D$$

Here β is full width half maxima and **Є** is the r.m.s strain in the material.

Scanning electron microscopy

The scanning electron microscopy (SEM) is a powerful non-destructive technique to study the topography, morphology and composition of the materials with much higher resolution. When a beam of highly energetic electrons strikes the sample, the secondary electrons, x-rays and back-scattered electrons are ejected from the sample. These electrons are then collected by the detector and convert into signal that displays on a screen. In the present study, the SEM micrograph was taken on the scanning electron microscope (JEOL-330 scanning microscope JEOL). As the samples are non-conducting, a thin layer of platinum is coated using a sputter coater.

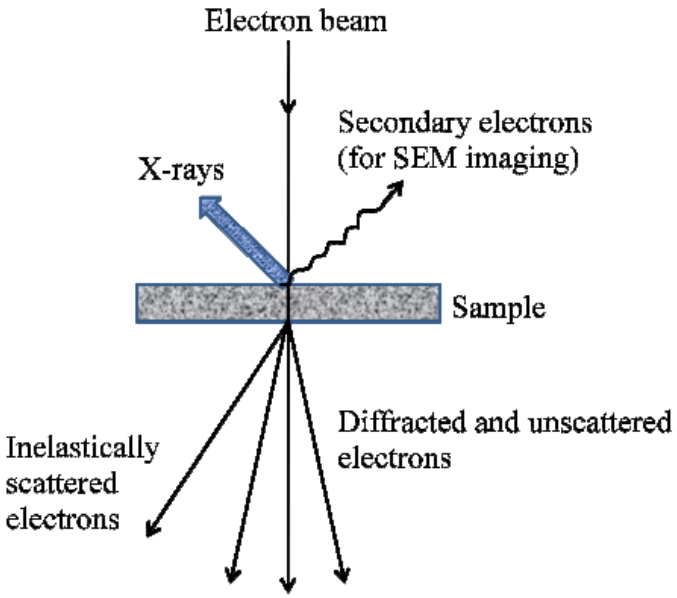

(Figure-2 Interaction of electron beam with specimen)

Dielectric Study

When a dielectric material is subjected to an external electric field, material becomes polarized due to induced dipole and permanent moments. The polarization is directly proportional to the macroscopic field i.e.

$$\mathbf{P} = \alpha \mathbf{E}$$

Here α is the polarizabilty of atoms and molecules**.**

Types of polarizations are

1. Electronic polarization
2. Atomic or ionic polarization
3. Dipolar polarization
4. Interface or space charge polarization

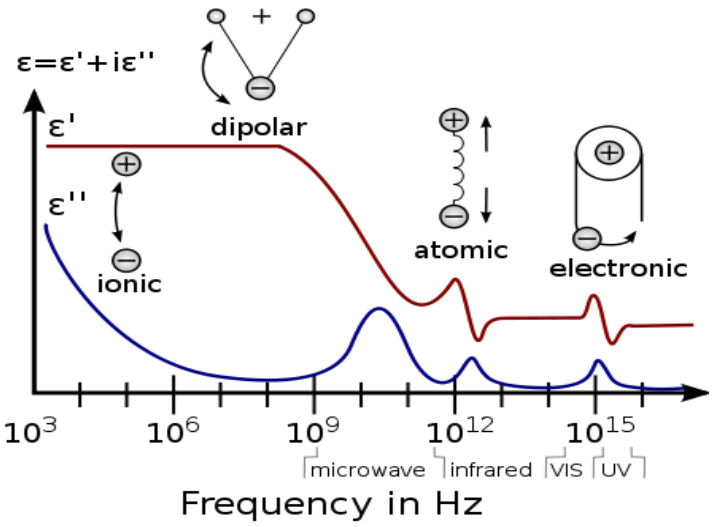

(Figure-3 Frequency dependence of dielectric constant)

When a dielectric is subjected to the ac voltage, the electrical energy is absorbed by the material and is dissipated in the form of heat. The dissipation is called dielectric loss (D).

In this work , to measure the relative permittivity (dielectric constant) and dielectric loss PSM 1735 was used .The electroded samples were used to make the measurements. The PSM was interfaced with the computer and the data (capacitance and D factor) was collected as a function of temperature at different frequencies. The measured capacitance was then converted into dielectric constant using the following formula:

$$C = \varepsilon_0 \varepsilon_r A / d$$

$$\varepsilon_r = C\ d / \varepsilon_0\ A$$

Where, C: Capacitance in farad (F)

ε: Permittivity of free space in farad per meter (8.85 x 10 -12 F/m)

ε r : Dielectric constant or relative permittivity of the sample.

A : Area of each plane electrode in square meters (m 2)

d : Separation between the electrodes in meters (m)

In the present study, we have taken data using PSM-1735 impedance analyzer.

Chapter-3

Result and Discussion

3.1 Structural analysis

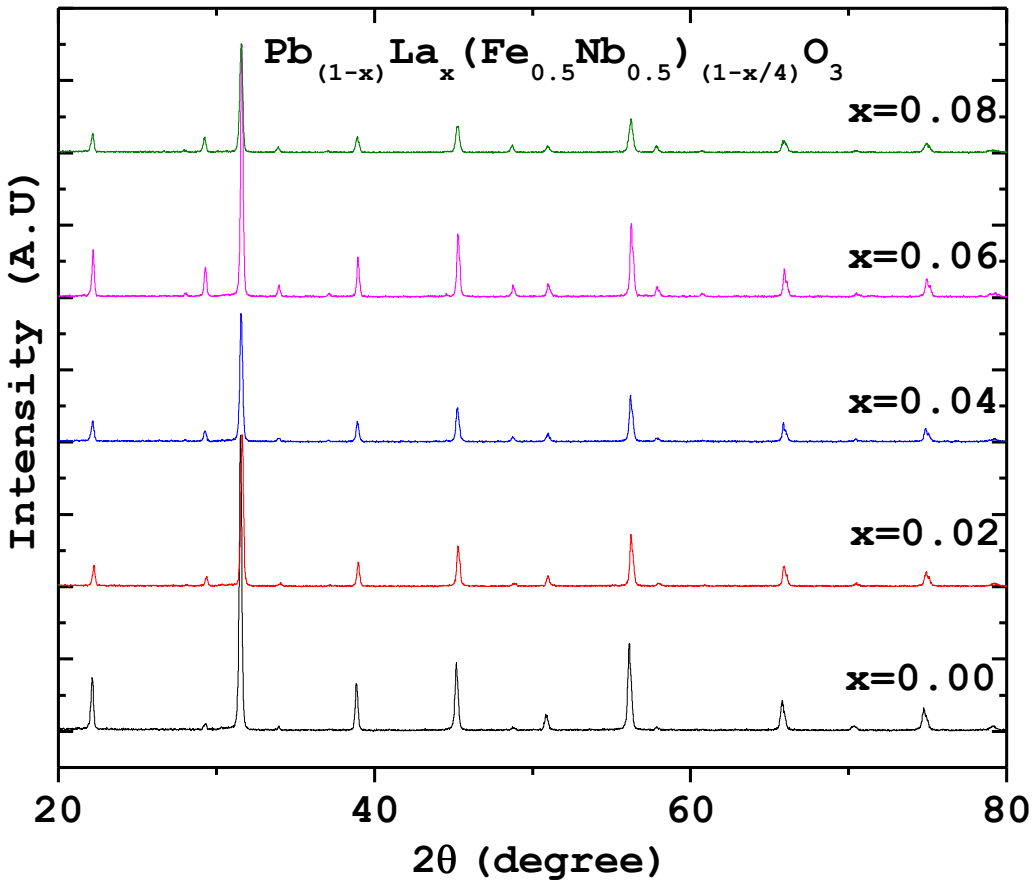

(Figure.1 X-ray diffraction pattern of $Pb_{(1-x)}La_x(Fe_{0.5}Nb_{0.5})_{(1-x/4)}O_3$ (x=0.00,0.02,0.04,0.06,0.08) at room temperature)

Figure 1 compares the room temperature XRD patterns of calcined powder of $Pb_{(1-x)}La_x(Fe_{0.5}Nb_{0.5})_{(1-x/4)}O_3$ (x=0.00, 0.02, 0.04, 0.06, 0.08). The diffraction pattern is different from that of ingredients suggest the formation of new compounds with a presence of small amount of secondary Phase (around the peak position of 27^o). It has also been observed that, there is a

change in the peak position, peak intensity and peak shape of PFN on increasing La concentration. The peak position full width at half maximum FWHM (β), and intensity of each peak were calculated using commercially available software (PEAK FIT). Indexing of XRD patterns was carried out using diffraction angle (2θ) and intensity value of each peak by a standard IUCR software ***CHECK-CELL [15]***. The best agreement in observed and calculated 2ɵ (i.e., $\Delta\theta$ ($2\theta_{obs}$-2 $_{cal}$) = minimum) for monoclinic system (Table-1). The crystal structure was found to be monoclinic for all compositions. The lattice parameters, unit cell volume, of the samples are listed (Table-2).The lattice parameters were observed to be decrease with increase in La concentration.

Table-1 Comparison of observed and calculated 2θ-values, miller indices of La+3 modifies Lead iron niobate.

$Pb_{(1-x)}$ La_x $(Fe_{0.5}$ $Nb_{0.5})_{(1-x/4)}O_3$ x=0.00						
Sl No.	2θ(observed) degree	2θ(calculated) degree	2θ difference	h	k	l
1	22.1344	22.1357	-0.0013	0	0	1
2	31.5138	31.4979	0.0159	2	0	0
3	38.8482	38.8370	0.0112	0	2	1
4	45.1709	45.1561	0.0148	0	0	2
5	50.7530	50.8009	-0.0479	-1	1	2
6	56.1055	56.0951	0.0104	0	2	2
7	65.8126	65.8299	-0.0173	2	2	2
8	70.3305	70.3272	0.0033	0	0	3
9	74.7229	74.7076	0.0153	-1	1	3

$Pb_{(1-x)}$ La_x $(Fe_{0.5}$ $Nb_{0.5})_{(1-x/4)}O_3$ x=0.02						
Sl No.	2θ(observed) degree	2θ(calculated) degree	2θ difference	h	k	l
1	22.2348	22.1780	0.0568	-1	1	0
2	31.6164	31.5551	0.0613	0	2	0
3	38.9645	38.9607	0.0038	2	0	1
4	45.2759	45.2461	0.0298	-2	2	0
5	50.9582	50.9709	-0.0127	2	2	1
6	56.2217	56.1961	0.0256	1	3	1
7	65.9011	65.8863	0.0148	0	4	0
8	70.4006	70.4054	-0.0048	1	3	2
9	74.8287	74.9018	-0.0731	-2	4	0

$Pb_{(1-x)}$ La_x $(Fe_{0.5}$ $Nb_{0.5})_{(1-x/4)}O_3$ x=0.04						
Sl No.	2θ(observed) degree	2θ(calculated) degree	2θ difference	h	k	l
1	22.0875	22.1322	-0.0447	0	0	1
2	31.5523	31.5505	0.0018	0	2	0
3	38.7717	38.8164	-0.0447	-2	0	1
4	45.2336	45.2003	0.0333	-2	2	0
5	50.9489	50.9088	0.0401	2	2	1
6	56.1892	56.1764	0.0128	1	3	1
7	65.8144	65.8506	-0.0362	2	2	2
8	70.4006	70.4254	-0.0248	0	4	1
9	74.7496	74.7166	0.0330	-1	1	3

$Pb_{(1-x)}$ La_x $(Fe_{0.5}$ $Nb_{0.5})_{(1-x/4)}O_3$ x=0.06						
Sl No.	2θ(observed) degree	2θ(calculated) degree	2θ difference	h	k	l
1	22.1666	22.1807	-0.0141	-1	1	0
2	31.5940	31.5574	0.0366	0	2	0
3	38.8508	38.8773	-0.0265	0	2	1
4	45.2734	45.2519	0.0215	-2	2	0
5	50.8698	50.8452	0.0246	1	1	2
6	56.2343	56.1815	0.0528	1	3	1
7	65.8144	65.8374	-0.0230	2	2	2
8	70.4006	70.4371	-0.0365	0	4	1
9	74.9078	74.9162	-0.0084	3	3	1

$Pb_{(1-x)}$ La_x $(Fe_{0.5}$ $Nb_{0.5})_{(1-x/4)}O_3$ x=0.08						
Sl No.	2θ(observed) degree	2θ(calculated) degree	2θ difference	h	k	l
1	22.0875	22.0962	-0.0087	0	0	1
2	31.5556	31.5483	0.0073	0	2	0
3	38.7717	38.7849	-0.0132	-2	0	1
4	45.2455	45.2171	0.0284	-2	2	0
5	50.8698	50.8322	0.0376	1	1	2
6	56.1676	56.1725	-0.0049	1	3	1
7	65.8144	65.8465	-0.0321	2	2	2
8	70.4006	70.4061	-0.0055	0	4	1
9	74.9078	74.9054	0.0024	3	3	1

The broadening in the X-ray line profile is mainly due to small crystallite size and anisotropic strain. Since both the effects are independent of each other we can separate out by Williamson–Hall method.

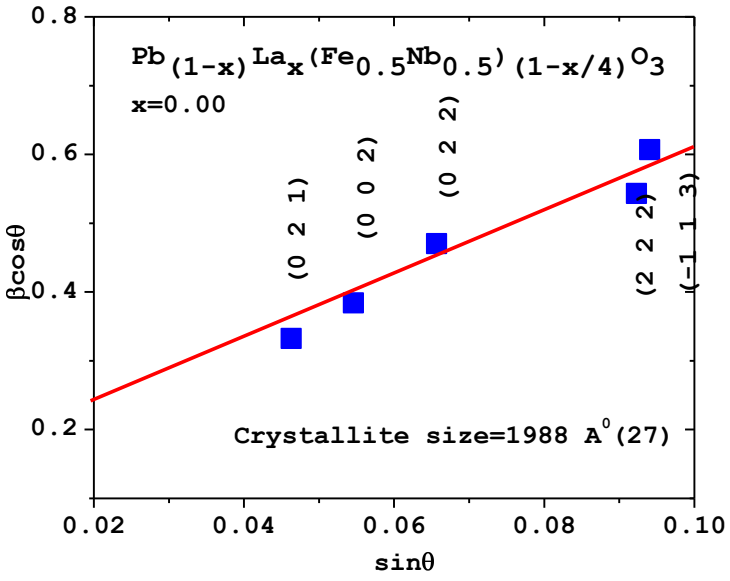

(**Figure2.**Williamson–Hall plot of PFN)

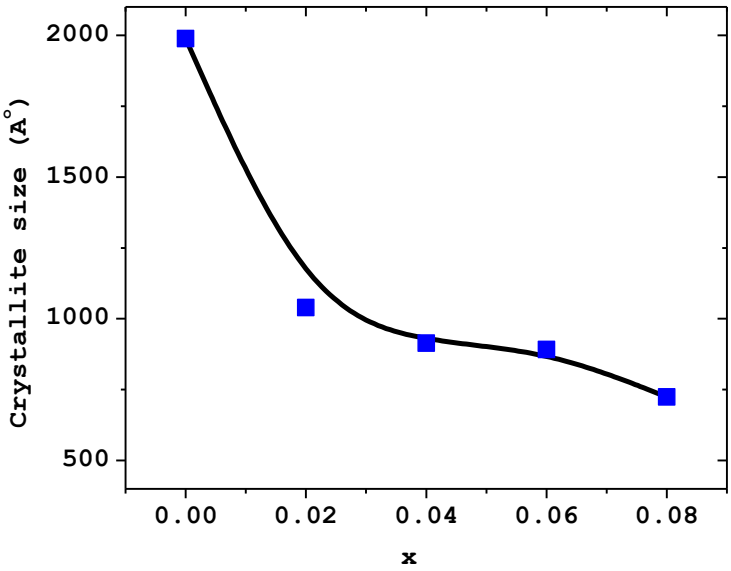

(**Figure3.** crystallite size dependence on x)

Williamson-Hall equation

$$\beta \cos\theta = 4\epsilon \sin\theta + \lambda/D$$

Here D crystallite size, λ wavelength used Є r.m.s strain in the samples.

By plotting βcos θ vs. sinθ. r. m. s. strain can be calculated from the slope and the crystallite size can calculated from the ordinate intercept Crystallite size decreases with increase in La incorporation at Pb site of PFN.

Table-2

Composition (x)	a(A°)	b(A°)	c(A°)	α= γ	β (degree)	Crystallite size (A°)
0.00	5.6805(44)	5.6800(47)	4.0157(09)	90	90.14	1988
0.02	5.6764(20)	5.6704(30)	4.0206(15)	90	90.13	1039
0.04	5.6764(63)	5.6712(29)	4.0163(22)	90	90.11	914
0.06	5.6754(84)	5.6700(27)	4.0179(63)	90	90.02	891
0.08	5.6721(33)	5.6716(17)	4.0228(23)	90	90.20	724

3.2 Scanning electron microscopy (SEM)

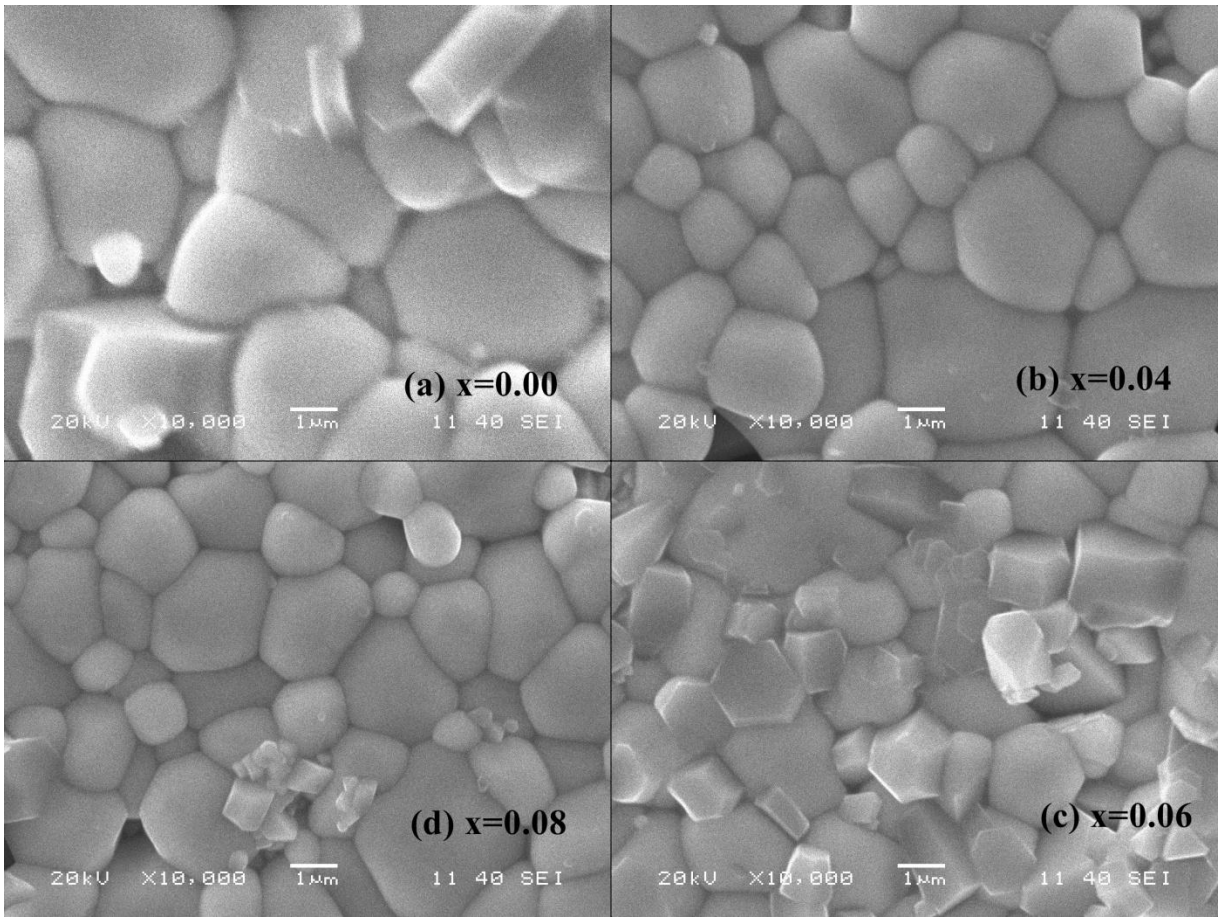

(**Figure4** Room temperature SEM micrographs of $Pb_{(1-x)}La_x(Fe_{0.5}Nb_{0.5})_{(1-x/4)}O_3$ (x=0.00,0.04,0.06,0.08))

The SEM micrographs show the polycrystalline nature of microstructure where grain sizes are inhomogeneously distributed throughout the sample with certain degree of porosity. The grain and grain boundaries are clearly distinct. The average grain size decreases with increase in La concentration at Pb site as observed by visual examination. The average grain size distributions of the samples were found to be 7μm to 3μm.

3.3 Dielectric Study

Figure 5. Shows the temperature dependence of dielectric constant for La modified PFN ceramics from room temperature to 250^{o}C at few selected frequencies with oscillation amplitude of 1V. It is observed that ε_r decreases monotonically on increasing frequency at all the temperatures, which represents the behavior of polar dielectric materials. It can be seen from the graph that εr increases with increase in temperature, attains its maximum value (ε_{max}) and then decreases. This observed dielectric anomaly shifts toward lower temperature with increase in La concentration from x=0.00 to 0.02 and falls below the room temperature for x=0.04, 0.06, 0.08. This dielectric anomaly is observed for La-modified PFN represents the ferroelectric – paraelectric phase transition which is diffuse type. It is also observed that dielectric constant decreases with increase in La substitution at Pb site which may be due to turning off of polarizibility of Pb in PFN. The above observation is related to the decrease of grain size due to the La^{3+} ions doping as observed from SEM. It is observed that for all the samples tanδ increases on increasing temperature with one anomaly in the temperature range 50-200^{o}C .This anomaly in tanδ shifting towards the high temperature side and the broadening of the peak increases with increase in frequency The reason for increase in tanδ at high temperature (in ceramics) can be attributed to the space charge polarization .Rapid increase in tan D at high temperatures is attributed to increase in electrical conductivity.

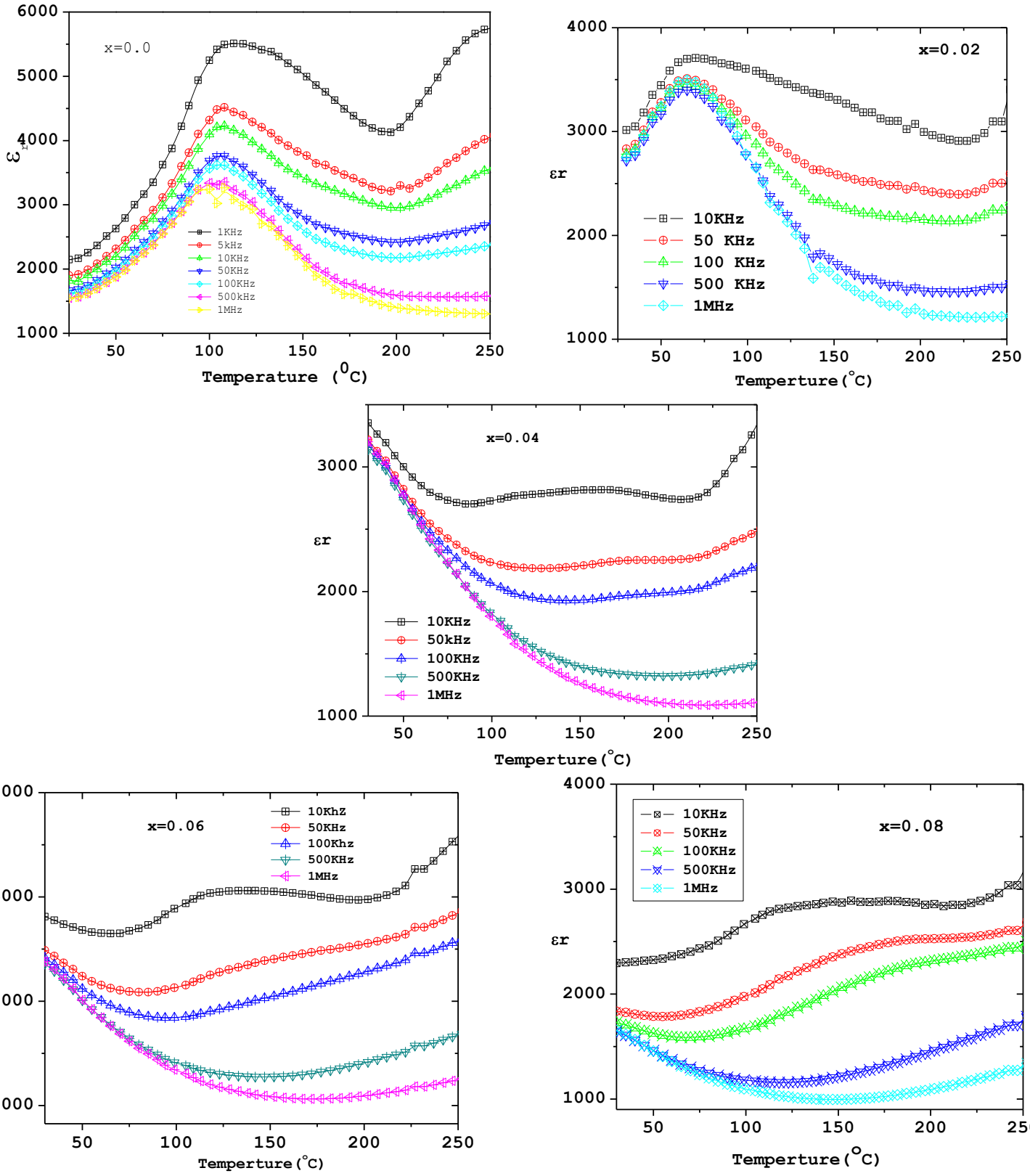

Figure5. Temperture dependent dielectric constant for $Pb_{(1-x)}La_x(Fe_{0.5}Nb_{0.5})_{(1-x/4)}O_3$ (x=0.00,0.02,0.04,0.06,0.08)

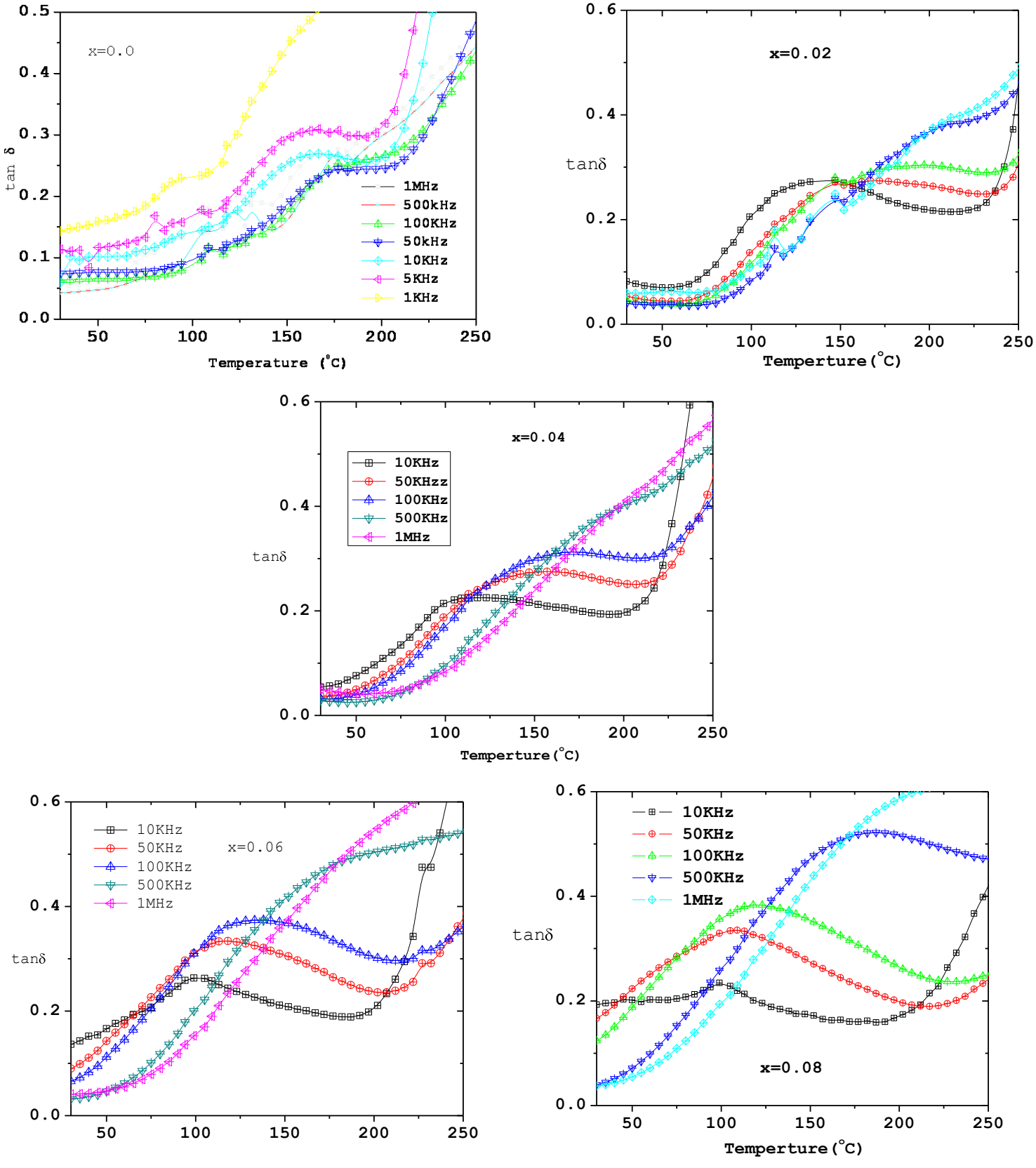

Figure6. Temperture dependence of dielectric loss (tanδ) for $Pb_{(1-x)}La_x(Fe_{0.5}Nb_{0.5})_{(1-x/4)}O_3$ (x=0.00,0.02,0.04,0.06,0.08)

Conductivity studies

Figure 7. Shows the variation of ac electrical conductivity (σ_{ac}) of PFN as a function of frequency at different temperatures and for all La modified PFN ceramics. The ac conductivity was calculated using the relation $\sigma_{ac} = \varepsilon_o\varepsilon_r\omega \tan\delta$. In the low frequency region, ac conductivity remains almost constant (i.e. frequency independent plateau region, representing d.c conductivity) whereas the dispersion of conductivity was observed in the higher frequency region. The crossover from the frequency independent region to the frequency dependent regions represents the onset of the conductivity relaxation, indicating the transition from long range hopping to the short-range ionic motion in the material. The frequency dependence of ac conductivity obeys Jonscher's power law, i.e. $\sigma_{ac} = \sigma_0 + A\omega^n$, where σ_0 is frequency independent conductivity (which is related to dc conductivity), A is the temperature dependent pre-exponential factor and n is frequency exponent, ($0 < n < 1$). As ac conductivity increases with rise in temperature, all the compounds have negative temperature coefficient of resistance (NTCR) behavior typically semiconducting behavior.

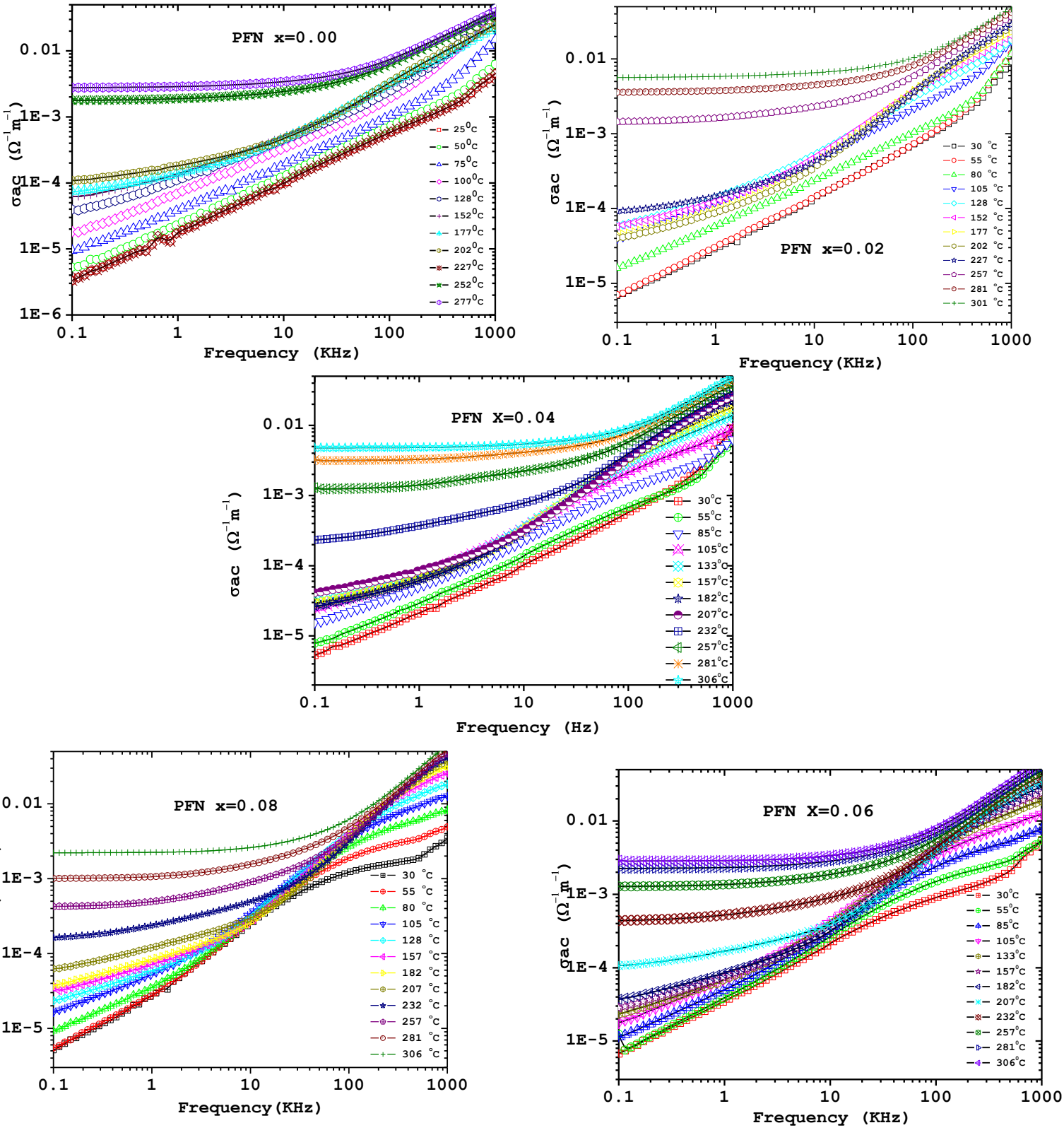

Figure7. **V**ariation of σ_{ac} with frequency for $Pb_{(1-x)}La_x(Fe_{0.5}Nb_{0.5})_{(1-x/4)}O_3$ (x=0.00,0.02,0.04,0.06,0.08)

3.4. Impedance Spectroscopic studies

Figure 8. represents the temperature dependent complex impedance (Nyquist plot) of La-modified PFN ceramics. The linear variation of $Z^{//}$ with $Z^{/}$ in the complex impedance plot in low temperature range from room temperature to 200°C indicates the insulating properties of the material. Above 200 °C, circular arc formation trend started which is due to the increase of conductivity. The impedance plots seem to have two overlapped semicircles. Each semicircle of the Nyquist plot corresponds to the different contribution to the electrical response. The high frequency semicircle can be attributed to the bulk (grain) property and low range frequency corresponds to grain boundary property of the material .The relaxation process associated with this observation is non-ideal in nature. This origin of non-Debye type behavior may be due to several factors such as grain orientation, grain size distribution, grain boundaries, atomic defect distribution and stress–strain phenomena. The intercept of the semicircular arc on the real axis gives the dc resistance of the material. It is seen from that the dc resistance increases with increase in the La content.

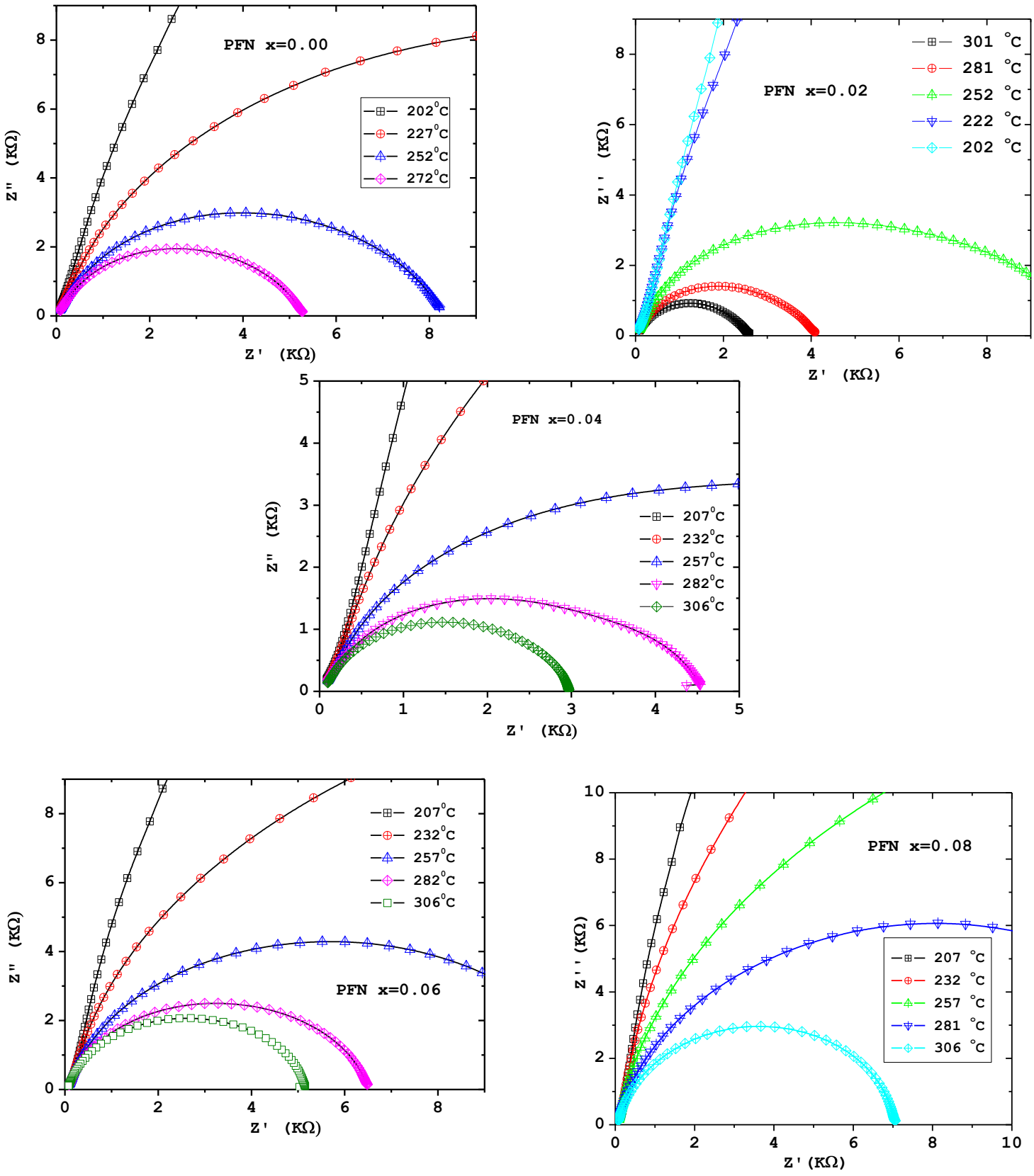

Figure8. Nyquist plot for $Pb_{(1-x)}\ La_x\ (Fe_{0.5}\ Nb_{\ 0.5})_{(1-x/4)}O_3$ (x=0.00,0.02,0.04,0.06,0.08)

Conclusions

In the present investigation, we have prepared the La+3 modified lead iron niobate perovskite ceramics having the general chemical formula $Pb_{(1-x)}\ La_x\ (Fe_{0.5}\ Nb_{\ 0.5})_{(1-x/4)}O_3$ (x=0.00, 0.02, 0.04, 0.06, 0.08) using high temperature solid state reaction route. The structural (XRD), microstructural (SEM) and electrical (dielectric and impedance) properties of the proposed compounds have been studied extensively.

Based on the results obtained following conclusions have been made.

(1) PFN and La-modified PFN samples were prepared by mixed oxide high temperature solid-state reaction route.

(2) X-ray diffraction (XRD) studies confirmed the formation of the compounds with monoclinic crystal system. Both the lattice parameters and crystallite size decreases with increase in La^{+3} concentrations.

(3) Scanning electron micrographs (SEM) of the compounds showed (1) polycrystalline nature of microstructure, (2) decrease in grain size with increase in La^{+3} concentration, (3) uniform distribution of grain size with high density.

(4) The ferroelectric to paraelectric phase transition temperature was found to be 115^{o}C for PFN and decreases with increase in La^{+3} substitution. For high concentration (i.e., x=0.04, 0.06 and 0.08) the phase transition temperature falls below the room temperature.

(5) The ac conductivity of the La-modified PFN obeyed the Jonsher's power law behavior.

(6) Complex impedance spectroscopy method has been used for better understanding of relaxation process and to establish relationship between the microstructure–electrical properties of the compounds.

References

1. J. Valasek, *Phys. Rev.B*, 15, 537- 538. (1920)
2. K. C. Kao, Dielectric phenomena in solids with emphasis on physical concepts of electronic processes. Elsevier Academic Press, (2004).
3. Safri, R. K. Panda, Victor F. Janas, "Ferroelectric Ceramics: Processing, Properties & Applications". Rutgers University, Piscataway NJ 08855, USA.
4. G Haertling. *Journal of American ceramic Society* 82, 797 (1999).
5. Jona & Shirane, Ferroelectric crystals, over publication New York.
6. Raymond et al. *Journal of Applied Phys.* 97, 084108(2005).
7. Wang et al. *Applied Physics Letters* 86, 192507(2005).
8. Kumar et al. *Applied Physics Letters* 60(1992).
9. Mishra et al. *Journal of physics. Condensed matter* 22(2010).
10. Sahoo t al. *Physica B*, 406(2011).
11. Singh et al. *Applied Physics Letters* 90,242915 (2007).
12. Cohen et al. *Physical Review B*, 42, (1990).
13. B. D. Cullity, S. R. Stock, Elements of X-Ray Diffraction. (3rd Edition) Prentice Hall, (2001).
14. Charles Kittel, Introduction to Solid State Physics, Wiley India Edition, 2008.
15. Dr Lachlan M.D. Cranswick, *CHECK CELL.-IUCR Software,* Domaine Universitaire BP 46, France.